



An architecture for a CBR image segmentation system

Petra Perner*

Institute of Computer Vision and Applied Computer Sciences, Arno-Nitzsche-Strasse 45, 04277, Leipzig, Germany

Received 1 February 1999; accepted 1 August 1999

Abstract

Image segmentation is a crucial step in extracting information from a digital image. It is not easy to set up the segmentation parameter so that it gives the best fit over the entire set of images that need to be segmented. **This paper proposes a novel method for image segmentation based on CBR.** It describes the whole architecture, as well as the methods used for the various components of the systems, and shows how the technique performs on medical images. © 1999 Elsevier Science Ltd. All rights reserved.

Keywords: Case-based reasoning; Image segmentation; Medical image analysis

1. Introduction

Image segmentation is a crucial step in extracting information from a digital image. **It is not easy to set up the segmentation parameter** so that it fits best over the entire set of images. **Most segmentation techniques contain numerous control parameters, which must be adjusted to obtain optimal segmentation performance.** The parameter selection is usually done on a large enough test data set, which should represent the entire domain well enough in order to be able to build up a general model for the segmentation. However, it is often not possible to obtain a large enough data set and **therefore the segmentation model does not fit the entire data set, and needs to be adjusted to new data.** Note that a general model does not guarantee the best segmentation for each image; rather, it guarantees an average best fit over the entire set of images.

Another aspect of the problem is related to changes in image quality caused by variations in environmental conditions, image devices, etc. Thus **the segmentation performance needs to be adapted to these changes in image quality.** All this suggests using CBR for image

segmentation. A CBR framework has, indeed, been successfully used for the high-level unit of an image interpretation system (Perner, 1993, 1998a,b) and has demonstrated extraordinarily good performance in image interpretation compared to other approaches. Grimnes and Amond (1996) used CBR for medical image understanding based on a propose–verify–critique–modify framework which expands the idea of hypothesis-test based systems like Ernest (Kummert et al., 1993) by including a learning component.

This paper proposes a novel image-segmentation scheme based on case-based reasoning. The approach does not rely on a propose–verify framework; rather, **CBR is used to select the segmentation parameter according to the current image characteristics.** By taking account of both non-image and image information; the complex solution space is broken down in a subspace of relevant cases, where the variation in image quality between the cases is limited. It is assumed that images having similar image characteristics will show similar good segmentation results when the same segmentation parameters are applied to these images.

The method has been evaluated on a set of medical images **(CT scans of the brain)** where **the variations between the images and the objects in the images are naturally very high.** The complexity of the brain CT-scans is due to partial volume effects, which disturb

* Fax: +49 341 8665 636.

E-mail address: ibaiperner@aol.com (P. Perner).

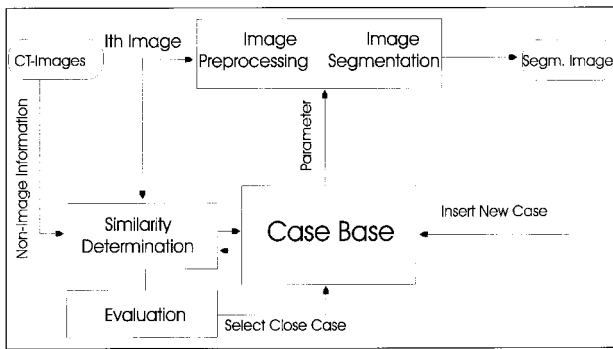


Fig. 1. Case-based reasoning unit.

the edges and produce contrast degradation by spatial averaging, and to typical problems such as patient movements, beam hardening, and reconstruction artifacts. These image characteristics are responsible for the over- and undersegmented results observed when unsupervised segmentation is applied.

We use the proposed method for labeling brain and liquor areas in CT slices. Based on this, brain/liquor ratio is calculated, which is a parameter used to determine the degree of degenerative brain diseases (Bettin et al., 1997).

Section 2 of the paper, describes the overall architecture. The case description is presented in Section 3. The segmentation algorithm is described in Section 4. The similarity measures for the non-image information and the image information are described in Section 5. Results are given in Section 6. Finally, conclusions are given in Section 7.

2. Overall architecture

The overall architecture can be divided into the image segmentation unit based on case-based reason-

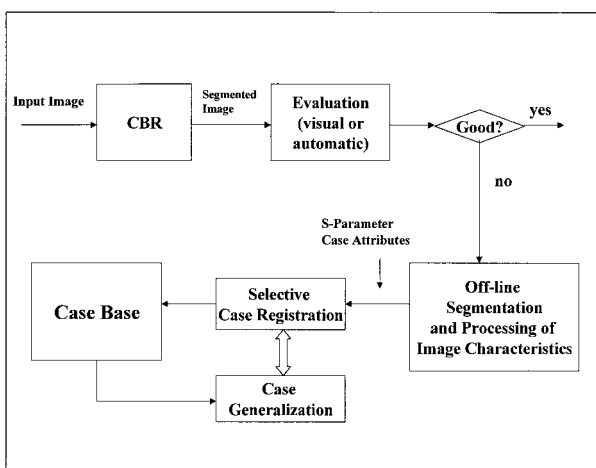


Fig. 2. Management of the case-base.

ing (Fig. 1), and the unit for the case base management part (Fig. 2).

2.1. Case-based reasoning unit

The case-based reasoning unit for image segmentation consists of a case base in which formerly processed cases are stored. A case comprises image information, non-image information (e.g. image acquisition parameters, object characteristics, etc.), and image-segmentation parameters. The task is now to find the best segmentation for the current image by looking in the case base for similar cases. Similarity determination is based on both non-image information and image information. The evaluation unit will take the case with the highest similarity score for further processing. If there are two or more cases with the same similarity score, the case to appear first will be taken. After the closest case has been chosen, the image-segmentation parameters associated with the selected case will be given to the image-segmentation unit, and the current image will be segmented (see Fig. 1). It is assumed that images having similar image characteristics will show similar good segmentation results when the same segmentation parameters are applied to these images.

The discussion that follows will assume the definition of regions based on constant local image features to be used for segmentation, the classification of regions into two object classes (brain and liquor), for labeling.

In the approach used for brain/liquor determination, the volume data of one patient (a sequence of a maximum of 30 CT-image slices) is given to the CBR image-segmentation unit. The CT images are stored in DICOM-format. Each file consists of a header and the image matrix. The header contains stored information about the patient and the image acquisition. The images are processed, slice by slice, before the brain/liquor volume ratio can be calculated. First, each image is preprocessed in order to eliminate the non-interesting image details, like the skull and the head shell, from the image. Afterwards, the non-image information is extracted from the image file header (see Section 3.1). From the image matrix contained in the DICOM-file, the statistical features describing the image characteristics are processed (see Section 3.2). This information, together with the non-image information, is given to the unit that determines the similarity. The similarity between the non-image information and the image information of the current case and the cases in case base is calculated (see Section 5). The closest case is selected, and the segmentation parameters (see Section 4) are given to the segmentation unit. The segmentation unit takes the parameters, adjusts the segmentation algorithm and

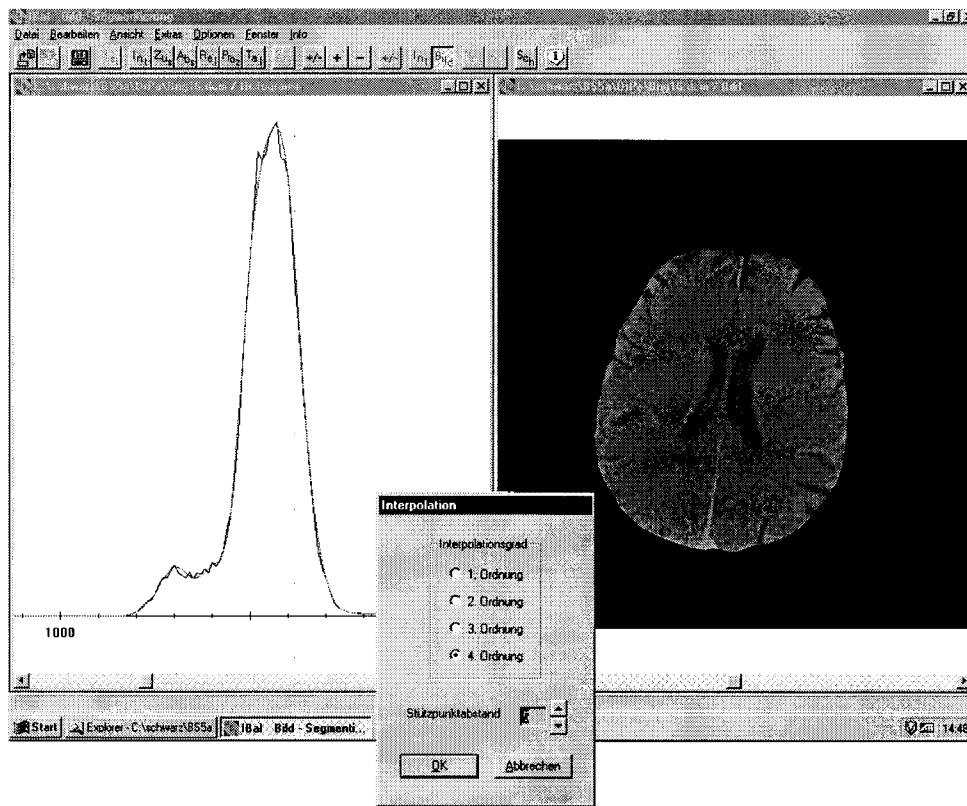


Fig. 3. User interface of the modification unit.

segments the image into brain and liquor areas. The resulting liquor area is displayed on screen to the user by red coloring over the area in the original image. This is done in order to give the user visual control of the result.

These processing steps are done slice by slice. After each slice has been processed, the volume for brain and liquor is calculated. Finally, the brain/liquor volume ratio is computed and displayed to the user.

2.2. Management of the case base

The result of the segmentation process is observed by a user. He compares the original image with the labeled image on display. If he detects deviations of the marked areas in the segmented image from the object area in the original image that should be labeled, then he will evaluate the result as incorrect, and case-base management will start. This will also be done if no similar case is available in the case base. The proposed method is close to the critique-modify framework described by Grimnes and Amond (1996).

The evaluation procedure can also be done automatically (Zhang, 1997). However, the drawback is that no general procedure is available; it can only be done in a domain-dependent fashion. Therefore, an automatic evaluation procedure would constrain the

use of the system. Once the user observes a bad result, he will tag the case as “bad case”. The tag describes the user’s critique in more detail. For the brain/liquor application it is necessary to know the following information for the modification phase: too much or too little brain area, too much or too little liquor area, and a similarity value less than a predefined value.

In an off-line phase, the best segmentation parameters for the image are determined, and the attributes that are necessary for similarity determination are calculated from the image. Both the segmentation parameters and the attributes calculated from the image are stored in the case base as a new case. In addition to that, the non-image information is extracted from the file header, and stored together with the other information in the case base. During storage, case generalization will be done to ensure that the case base will not become too large. Case generalization will be done by grouping the segmentation parameters into several clusters. Each different combination of segmentation parameters will be a cluster. The cluster name will be stored in the case together with the other information. Generalization will be done over the values of the parameters describing a case. In the current system, this function has not yet been fully realized, but has to be done manually by the knowledge

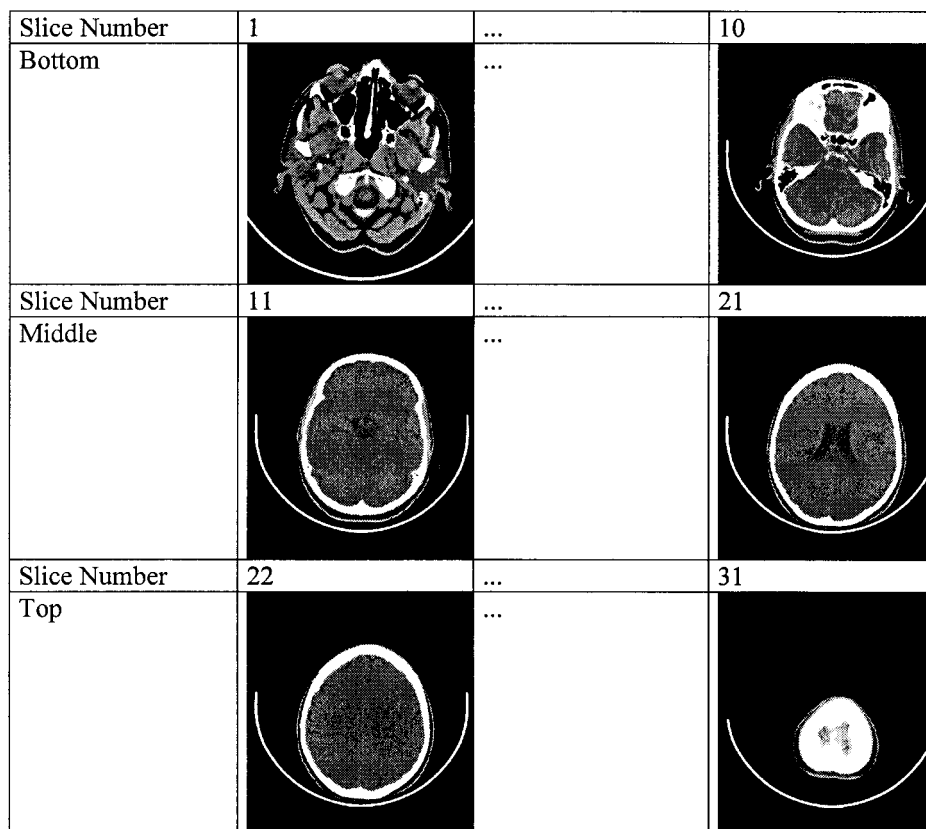


Fig. 4. CT images showing the different segments of the head.

engineer. The unit for modifying the segmentation is shown in Fig. 3.

3. Case structure and case base

A case consists of **non-image information, parameters describing the image characteristics** itself, and the solution (**the segmentation parameters**).

3.1. Non-image information

The non-image information necessary for this brain/liquor application will be described below. For other applications, different, appropriate non-image information will be contained in the case. For example, motion analysis (Kummer and Perner, 1999), involves the use of the camera position, relative movement of the camera and the object category itself as non-image information. For brain/liquor determination in CT-images, **patient-specific parameters** (like age and sex), **slice thickness** and **number of slices** are required. This information is contained in the header of the CT image file so that these parameters can be automatically accessed. Young patients have smaller liquor areas than old patients. The images therefore show different image characteristics. The anatomical struc-

tures (and therefore the image characteristics) also differ between women and men.

The number of slices may vary from patient to patient because of this biological diversity, and so may the starting position of the slices. Therefore, the numerical values are mapped onto three intervals: bottom, middle and top slices. These intervals correspond to the segments of the head of different image characteristics (see Fig. 4). The intervals can easily be calculated by dividing the number of slices by three. The remaining uncertainty in position can be ignored.

3.2. Image information

The kind of image information used to describe a case is closely related to the kind of similarity measure used for similarity determination. There is a lot of work going on at present in developing new measures for **comparing grey-scale images** (Zamperoni and Starovoitov, 1995; Wilson et al., 1997) for various objectives like image retrieval and **image evaluation.** **Before a decision was made to employ a particular similarity measure for this work, one of these new measures were evaluated against the measure already being used.** The reason for choosing one particular similarity measure, as well as the appropriate image in-

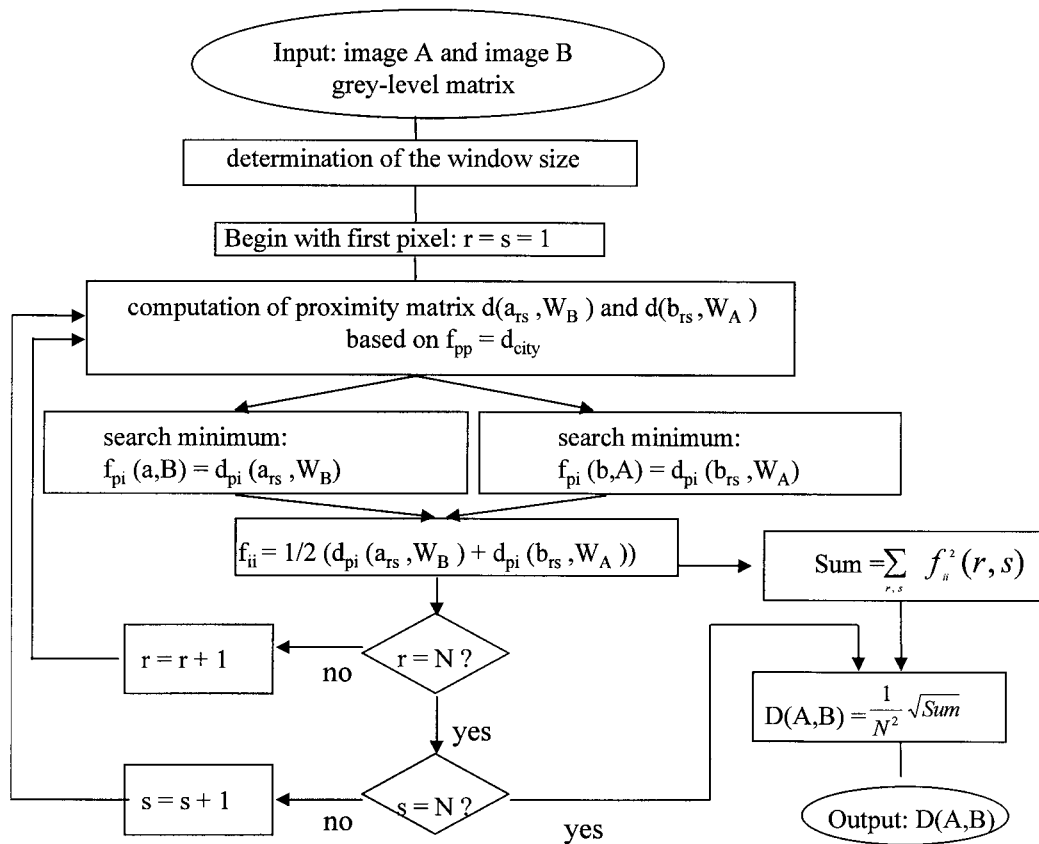


Fig. 5. Similarity determination by Zamperoni et al.

formation to describe a case, will be briefly discussed below.

3.2.1. IM1

The similarity measure developed by Zamperoni and Starovoitov (1995) can take the image matrix itself and calculate the similarity between two image matrices (see Fig. 5). The input to the algorithm is the two images that are being compared. According to the

specified distance function, the proximity matrix is calculated for one pixel at position r,s in image A to the pixel at the same position in image B , and to surrounding pixels within a predefined window. The same is done for the pixel at position r,s in image B . Then, clustering is performed, based on that matrix, in order to get the minimum distance between the compared pixels. Afterwards, the average of the two values is calculated. This is repeated until all the pixels of both

Table 1
Image features

Feature name	Calculation	Feature name	Calculation
Mean	$\bar{g} = \sum_g g \cdot H(g)$	Variance	$\delta_g^2 = \sum_g (g - \bar{g})^2 H(g)$
Skewness	$g_s = \frac{1}{\delta_g^3} \sum_g (g - \bar{g})^3 H(g)$	Curtosis	$g_k = \frac{1}{\delta_g^4} \sum_g (g - \bar{g})^4 H(g) - 3$
Variation coefficient	$\nu = \frac{\delta_g}{\bar{g}}$	Entropy	$g_E = - \sum_g H(g) \log_2 [H(g)]$
Centroid x	$\bar{x} = \frac{\sum_x \sum_y y \cdot x f(x, y)}{\sum_x \sum_y f(x, y)} = \frac{\sum_x \sum_y y \cdot x f(x, y)}{gS}$	Centroid y	$\bar{y} = \frac{\sum_x \sum_y y \cdot y f(x, y)}{\sum_x \sum_y f(x, y)} = \frac{\sum_x \sum_y y \cdot y f(x, y)}{gS}$
First order histogram	$H(g) = \frac{N(g)}{S}$	g = intensity value $N(g)$ = number of pixels of intensity value g in the image S = overall number of pixels	

*** H I E R A R C H I C A L C L U S T E R A N A L Y S I S ***

Dendrogram using Single Linkage
Euclidean measure used.

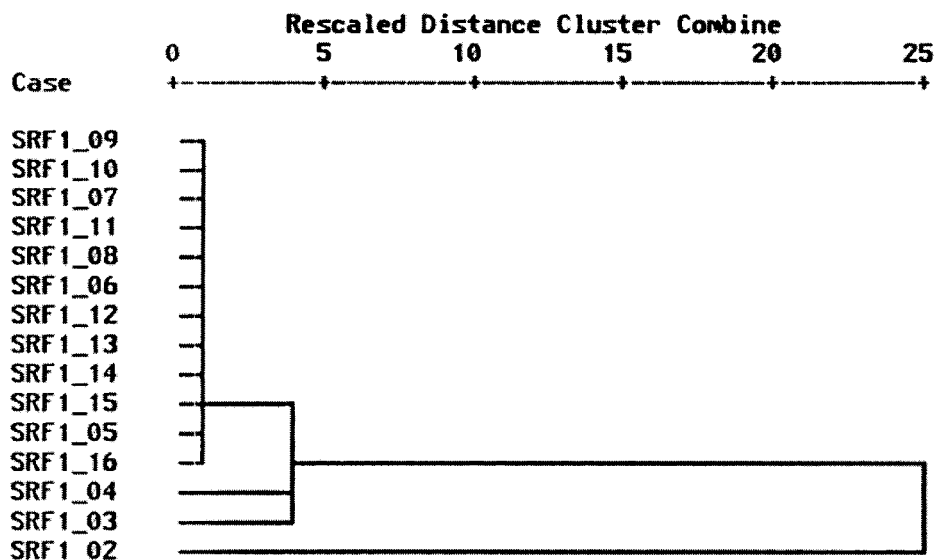


Fig. 6. Similarities between images of one patient based on IM1.

images have been processed. From the average minimal pixel distance, the final dissimilarity for the whole image is calculated. Use of an appropriate window should make this measure invariant to scaling, rotation and translation, depending on the window size.

For this kind of similarity determination, it is necessary to store the whole image matrix as the image-information for each case. However, the similarity measure based on Zamperoni's work has some drawbacks, which will be discussed later.

*** H I E R A R C H I C A L C L U S T E R A N A L Y S I S ***

Dendrogram using Single Linkage

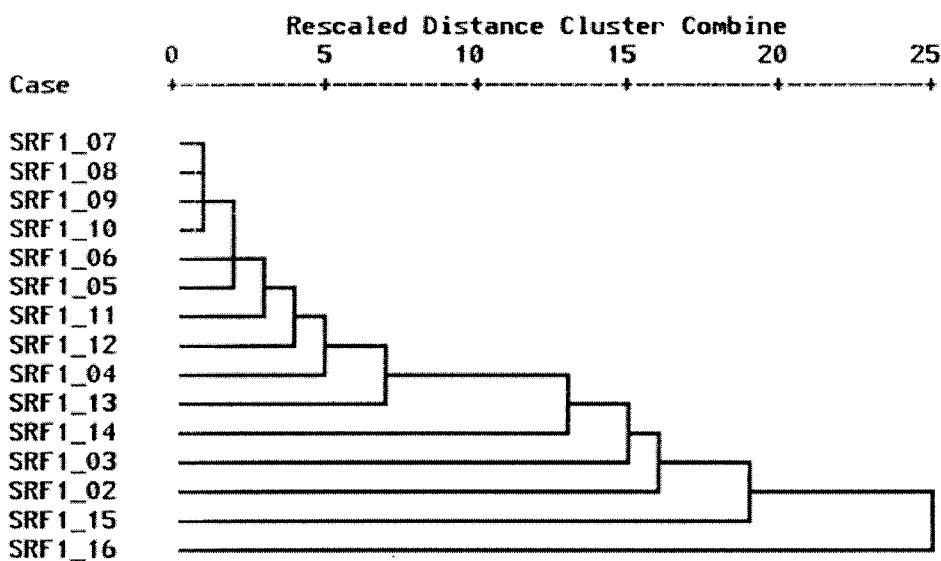


Fig. 7. Dendrogram of similarities between images of one patient based on IM2.

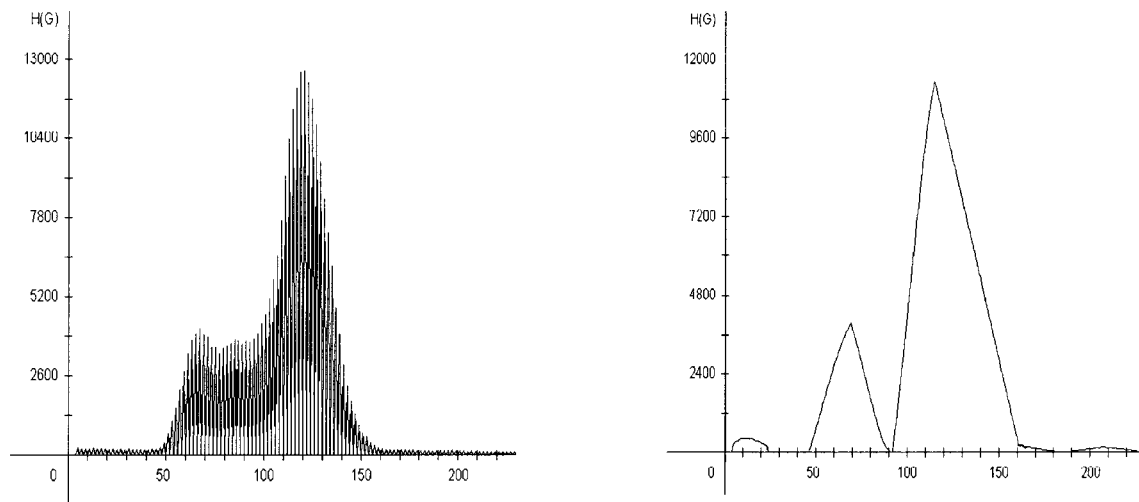


Fig. 8. Histogram of a CT-image and refined histogram.

3.2.2. IM2

A simpler approach is to calculate features from an image that will describe the statistical properties of the image. These features are statistical measures of the gray level, like mean, variance, skewness, kurtosis, variation coefficient, energy, entropy, and centroid (Dreyer and Sauer 1982) (see Table 1). The similarity between two images is calculated on the basis of these features.

3.2.3. Comparison of IM1 and IM2

Investigations were undertaken into the behavior of the two similarity measures. The similarities between the image slices of one patient are calculated, based first on IM1 and further on IM2. Each single-linkage method is then used to create a dendrogram, which graphically shows the similarity relation between the slices.

The dendrogram (see Fig. 6) based on IM2 shows two clusters: one for the slices in the middle and at the top of the head, and one for the slices at the bottom of the head. There is no clear cluster for the top and the middle slices. Nevertheless, the differences in the similarity values are big enough to make a distinction between these slices. The highest dissimilarity is recognized between the slices from the bottom, which happens because of the high complexity of the image structures in that sphere.

The dendrogram based on IM1 shows a finer graduation between the various slices (see Fig. 7). It can also distinguish better between the bottom, middle and top slices. However, slices from different patients are compared, it shows some drawbacks, which are caused by rotation, scaling and translation. The invariant behavior of this measure is related to the window size. Compensating for these effects requires a large window

size, which on the other hand causes high computation time (more than 3 min on a 4-node system based on Power PC 604 and a window size of 30×30 pixels). This makes this measure unsuitable for the problem, at hand.

3.2.4. Results

The similarity measure based on IM1 has limited invariance in the face of rotation, scaling and translation. Therefore, it was decided to use the similarity measure based on IM2. Moreover, in the case of IM1, it is necessary to store the whole image matrix as a case and calculate the similarity over the entire image matrix. The computational costs for the similarity calculation are very high, and so would be the storage capacity. The lower sensitivity of IM2 to the different sectors of the brain can be reduced by introducing the slice number as non-image information discussed in Section 3.1.

For the similarity measure based on IM2, it is only necessary to calculate features from the images before the cases can be stored in the case base. This calculation is of low computational cost. Each image is described by statistical measures of the gray level like: mean, variance, skewness, kurtosis, variation coefficient, energy, entropy, and centroid. This information, together with the non-image information and segmentation parameters, comprises a case.

4. Segmentation algorithm and segmentation parameters

The gray level histogram is calculated from the original image. This histogram is smoothed by some numerical functions and heuristic rules (Ohlander et al., 1978; Lee, 1986) to find the cut points for the liquor

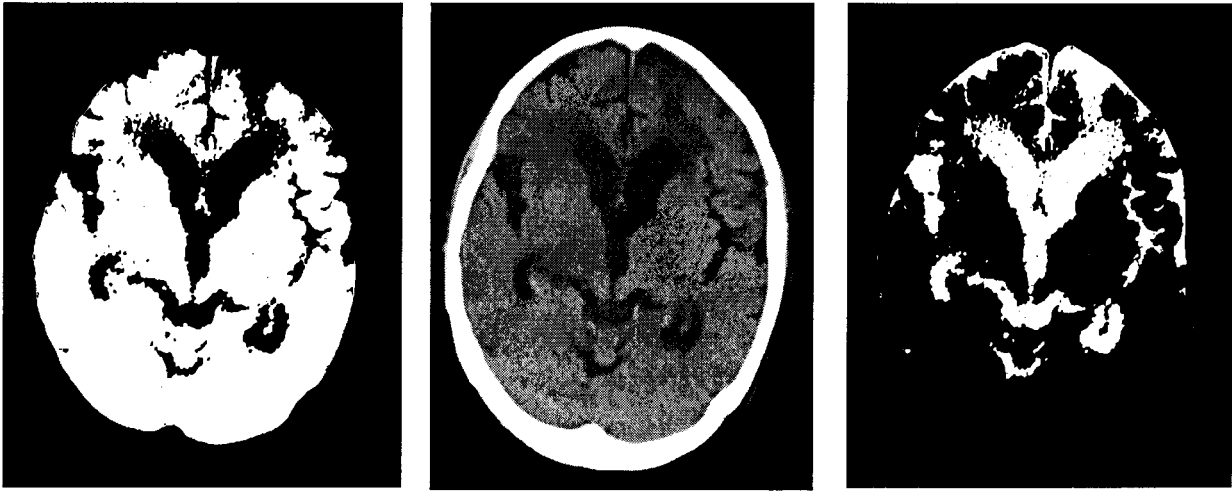


Fig. 9. Original and labeled image for brain and labeled image for liquor.

and brain gray-level areas. The parameters of the function and rules are stored with the cases, and given to the segmentation unit if the associated case is selected. The following steps are performed. The histogram is smoothed by a numerical function. There are two parameters to select: the complexity of the interpolation function and the interpolation width. Then the histogram is segmented into intervals, such that each begins with a valley, contains a peak and ends with a valley. The peak-to-shoulder ratio of each interval is tested first. An interval is merged with the neighbor sharing the higher of its two shoulders if the ratio of peak height to the height of its higher shoulder is greater than or equal to some threshold. Finally, the number of the remaining intervals is compared to a predefined number of intervals. If more than this have survived, the intervals with the highest peaks are selected. The number of intervals depends on the number of classes into which the image should be segmented. The thresholds are calculated and then applied to the image. Fig. 8 shows a histogram for an original image and the histogram after being processed by the algorithm. The original image and the resulting labeled images are shown in Fig. 9.

5. Similarity determination

Similarity comprises two parts: non-image similarity and image similarity. The final similarity is calculated by:

$$\text{Sim} = \frac{1}{2}(\text{Sim}_N + \text{Sim}_I) = \frac{1}{2}(S(C_I, b) + 1 - \text{dist}_{AB}). \quad (1)$$

It was decided that non-image and image similarity should have equal influence to the final similarity.

Only when both similarities have a high value, will the final similarity be high.

5.1. Similarity measure for non-image information

Tversky's similarity measure is used for the non-image information (Tversky, 1977). The similarity between a case C_i and a new case b presented to the system is:

$$S(C_i, b) = \frac{|A_i|}{\alpha |A_i| + \beta |D_i| + \chi |E_i|} \quad (2)$$

$\alpha = 1, \beta, \chi = 0.5$

with A_i , the features that are common to both C_i and b ; D_i , the features that belong to C_i but not to b ; E_i , the features that belong to b but not to C_i .

5.2. Similarity measure for image information

For the numerical data,

$$\text{dist}_{AB} = \frac{1}{k} \sum_{i=1}^K w_i \left| \frac{C_{iA} - C_{i \min}}{C_{i \max} - C_{i \min}} - \frac{C_{iB} - C_{i \min}}{C_{i \max} - C_{i \min}} \right| \quad (3)$$

is used, where C_{iA} and C_{iB} are the i th feature values of image A and B , respectively. $C_{i \min}$ is the minimum value of the i th numeric or symbolic feature. $C_{i \max}$ is the maximum value of the i th feature, and w_i is the weight attached to the i th feature with $w_1 + w_2 + \dots + w_i + \dots + w_k = 1$. For the first run, w_i is set to one. Further studies will deal with learning of feature weights.



Fig. 10. Screen display of the case-based brain/liquor system.

6. Results

6.1. Evaluation

The user interface of the current system is shown in Fig. 10. Three slices of the sequence of slices for one

patient are shown at the same time on the display. In chronological order a new slice from this sequence is processed, the images on the display are scrolled from right to left and the actual processed image is displayed at the right hand side of the screen. The original images are shown at the top of the display and

Table 2
Manual and automatic measures for brain/liquor for 9 patients

Case	In case base	Brain (cm ³)		Liquor (cm ³)		Brain/liquor ratio	
		Manual	Autom.	Manual	Autom.	Manual	Autom.
NNA	contain	1331.5	1197.89	287.76	316.98	4.63	3.78
WFH	contain	1211.2	1123.75	201.20	243.58	6.02	4.91
MRG	contain	1381.5	1078.20	314.51	346.13	4.39	3.12
HNH	part_cont	1097.3	1080.48	213.51	274.50	5.14	3.94
MRR	part_con	1152.8	1212.08	144.92	145.01	7.95	8.36
TRM	part_con	1420.0	1232.88	248.34	284.45	5.72	4.33
MEI	not_cont	983.0	986.31	147.95	180.27	6.64	5.47
MNH	not_cont	846.7	833.23	165.00	189.22	5.13	4.40

Comparison between Manual and Automatic Brain/Liquor Determination

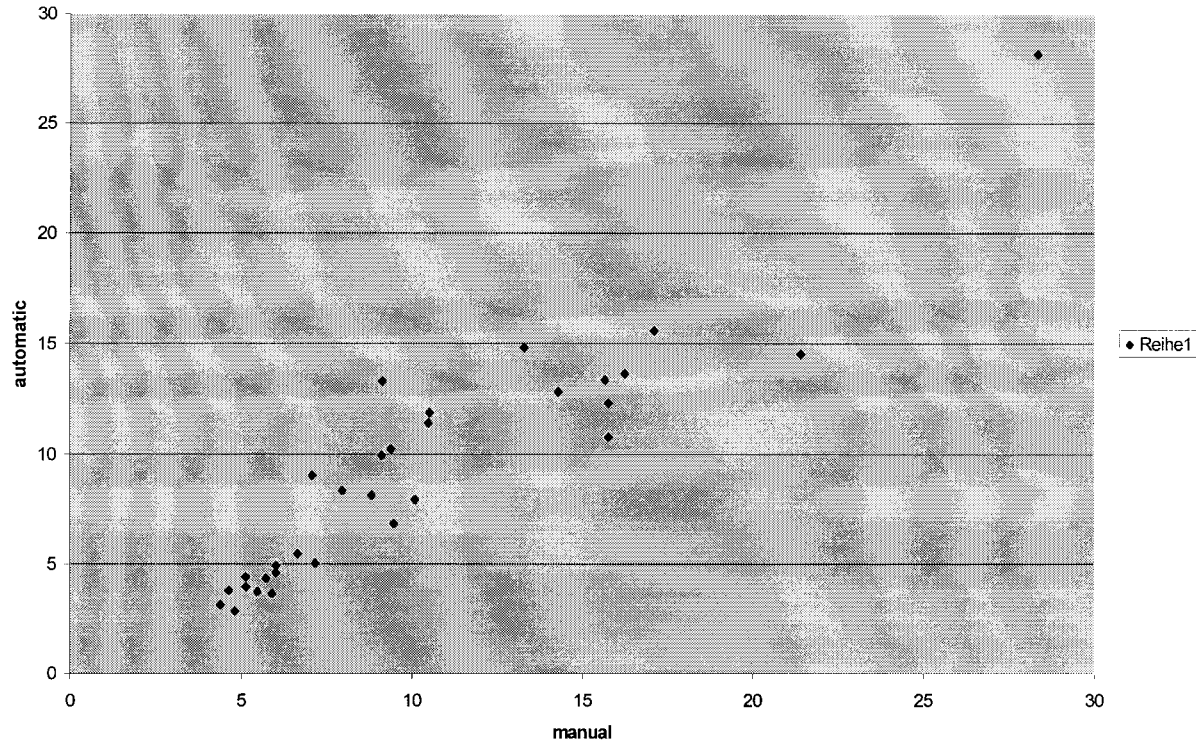


Fig. 11. Diagram of manual versus automatic results.

the labeled images are shown at the bottom of the display, so that the user can also compare the images visually. The system is in practical use by the medical department at the university of Halle. The system contains 130 cases in case base.

The performance of the system was assessed by comparing labeled images manually by the physicians with images automatically labeled by the system. Some of these images are contained in the case base, while others are not. In a BMFT study (1996), a physician from the University of Leipzig labeled the images of 30 patients by hand. For each patient there are approx. 20 images, giving a total of 600 images for evaluation. Images labeled by another physician from the University of Halle were also used. This physician labeled the images twice, to give an indication of measurement error when the task is done by a human.

Table 2 compares the manual results and the automatic results. The algorithm labels more liquor area than a human expert does. However, Fig. 11 shows a strong linear correlation between the results using the system and the results of a human expert ($r = 0.85$). This is a very good result.

6.2. Knowledge acquisition aspect

The case base has to be filled with a large enough

set of cases. As described above, the header of the DICOM-File contains the non-image information. This information can be automatically extracted from the file and stored in the case base. Likewise, the image information can be extracted from the image matrix contained in the DICOM-file. A little more effort is needed for the determination of the segmentation parameters. However, this task is efficiently supported by the acquisition unit shown in Fig. 3. The histogram is smoothed and processed, step by step, according to the implemented segmentation algorithm under the control of the knowledge engineer. The knowledge engineer can control each segmentation parameter and preview the segmentation results on screen. Once the best segmentation result has been reached, the chosen segmentation parameters are stored, together with the other information in the case base.

6.3. General comments

For the first time, a system is automatically delivering to the physicians, a measure for the brain/liquor ratio. The only thing that the physician has to do is to tell the system what images should be examined. No human interaction is necessary, as it is for other volumetric image analysis systems (Tschammler et al.,

1996). The system automatically delivers a measure back to the physician. In contrast to the recent qualitative examination of the CT images, a quantitative examination is possible which gives a valid measure and allows one to detect the graduation between different stages of a disease, and control of a patient over time.

7. Conclusion

This paper has presented a methodology for a CBR-based image-segmentation system. The system performs image segmentation by looking up a case base for similar cases and takes the segmentation parameters associated to the similar case in order to perform segmentation of the current image. The system was tested by comparing manually labeled images with automatically labeled images. The results show that by using the new method, good results for the brain/liquor ratio can be obtained. Since it is well known that a physician does not always know what he should label as brain and what as liquor, the difference in labeling between a human and the system is not a cause for. A good evaluation of the system would only be possible if there were to exist a true “gold standard”, which may become available if the work on simulation of the brain CT-images will shows good results.

This new system has given the user a fully automatic system, which needs no user interaction when calculating the brain/liquor ratio. Such a system gives the opportunity to replace a qualitative measure based on a subjective judgement, with a quantitative measure, which is reproducible.

Further work will be done on generalizing the cases and segmentation parameters and learning feature weights. In addition, the system will be extended to other volumetric tasks, for example the measurement of the volume of the human liver and liver metastases.

Acknowledgements

The author would like to thank Professor Heywang-Köbrunner and Dr Beck from the medical department of the University of Halle for the cooperation on this work. For providing the results of the BMFT study thanks are due to Professor Dietrich from the medical department of the University of Leipzig. Technical help by Mr Kraft is acknowledged.

References

Bettin, S., Dietrich, J., Dannenberg, C., Barthel, H., Zedlick, D.,

- Jobst, K., Knapp, W.H., 1997. Früherkennung von Hirnleistungstörungen — Vergleich linearer und volumetrischer Parameter (CT) mit Ergebnissen der Perfusions-SPET. In: Fortschritte auf dem Gebiet der Röntgenstrahlen 166, p. 89.
- BMFT, 1996. Study, Degenerative Erkrankungen des zentralen und peripheren Nervensystems — Klinik und Grundlage. Abschlußbericht der medizinische Fakultät der Uni Leipzig.
- Dreyer, H., Sauer, W., 1982. Prozeßanalyse. Berlin, Verlag Technik.
- Grimnes, M., Amond, A., 1996. A two layer case-based reasoning architecture for medical image understanding. In: Smith, I., Faltings, B. (Eds.), *Advances in Case-Based Reasoning*. LNAI 1168. Springer Verlag, Berlin, pp. 164–178.
- Kummer, G., Perner, P., 1999. Motion Analysis. IBAI Report, Leipzig.
- Kummert, F., Niemann, H., Prechtel, R., Sagerer, G., 1993. Control and explanation in a signal understanding environment. *Signal Processing* 32, 111–145.
- Lee, C.H., 1986. Recursive region splitting at the hierarchical scope views. *Computer Vision Graphics, and Image Processing* 33, 237–259.
- Ohlander, R., Price, K., Reddy, D.R., 1978. Picture segmentation using recursive region splitting method. *Computer Graphics and Image Processing* 8, 313–333.
- Perner, P., 1993. Case-based reasoning for image interpretation in non-destructive testing. In: Richter, M. (Ed.), *The First European Workshop on Case-Based Reasoning*, vol. II. SFB 314 Univ, Kaiserslautern, pp. 403–410.
- Perner, P., 1998a. Different learning strategies in a case-based reasoning system for image interpretation. In: Smith, B., Cunningham, P. (Eds.), *Advances in Case-Based Reasoning*. LNAI 1488. Springer, Berlin, pp. 251–261.
- Perner, P., 1998b. Using CBR learning for the low-level and high-level unit of a image interpretation system. In: Sameer, S. (Ed.), *International Conference on Advances Pattern Recognition ICAPR98*. Springer, London, pp. 45–54.
- Tschammler, A., Middendorf, C., von Lüdinghausen, M., Krahe, Th., 1996. Computerized tomography volumetry of cerebrospinal fluid by semiautomatic contour recognition and gray value histogram analysis. *Rofo Fortschritte auf dem Gebiet der Roentgenstrahlen und neuen bildgebenden Verfahren* 164 (1), 13.
- Tversky, A., 1977. Feature of similarity. *Psychological Review* 84 (4), 327–350.
- Wilson, D.L., Baddeley, A.J., Owens, R.A., 1997. A new metric for grey-scale image comparison. *International Journal of Computer Vision* 24 (1), 1–29.
- Zamperoni, P., Starovoirov, V., 1995. How dissimilar are two gray-scale images. In: *Proceedings of the 17th DAGM Symposium*. Springer, Berlin, pp. 448–455.
- Zhang, S., 1997. Evaluation and comparison of different segmentation algorithm. *Pattern Recognition Letters* 18 (10), 963–968.

Petra Perner received her Diploma degree in 1981 from the Technical University of Mittweida. From 1981 to 1985, she worked as research assistant in the research group “Industrial robot control” at the Technical University of Mittweida. She received her Ph.D. degree in Computer Science in 1985. From 1985 to 1991, she has been working at the Technical University of Leipzig. From 1986 to 1990, she was the head of the research group “Opto-electronical Inspection Systems”. In 1991, she was a visiting scientist at the Fraunhofer-Institute of Non-Destructive Testing in Saarbrücken. In 1992, she worked as a visiting scientist at IBM T.J. Watson Research Center Yorktown Heights, USA. From 1993 to 1995, she has been a Scientist and Lecturer at the HTWK Leipzig. Since 1995, she has been the director of the Institute of Computer Vision and Applied Computer Sciences in Leipzig. Her research interests are image interpretation, machine learning, case-based reasoning, image database and data mining.